Int. J. Heat Mass Transfer. Vol. 29, No. 4, pp. 549–554, 1986
Printed in Great Britain

0017–9310/86 $3.00 + 0.00
Pergamon Press Ltd.

Melting of powder grains in plasma spraying

I. GROMA and B. VETŐ
Institute for General Physics, Loránd Eötvös University, Budapest, Hungary

(*Received* 24 *May* 1985)

Abstract—A numerical model of the melting of small particles entered in a free DC plasma jet was studied to predict the optimal parameters of plasma spraying. The equation of motion for the solid/liquid interface inside a particle passing through a plasma jet was determined and its numerical solution was given in some special cases. The strong temperature and velocity variation inside the plasma jet and the temperature dependence of the plasma parameters were taken into account.

1. INTRODUCTION

IN THE use of plasma spraying the basic condition is that the particles become fully molten but not overheated during their flight. In such cases the powder particles can be spread on the substrate and the porosity of the coated deposit is low. Therefore it is important to know the conditions of full melting of a particle in plasma.

One possibility to take into account these conditions is to suppose that the thermal conductivity of powder grains is so high that the temperature gradient inside the particles can be neglected [1–5]. According to Houben [5] this assumption can be used when

$$\frac{\kappa}{\kappa_g} \ln\left[\frac{T_g - T_r}{T_g - T_s}\right] > 0.9 \qquad (1)$$

where κ and κ_g are the thermal conductivity of the powder and the plasma, T_g and T_s are the temperatures of the plasma and the powder surface, respectively, and T_r is the room temperature. This connection is not satisfied, however, for many materials (e.g. Al_2O_3).

Another possibility is the numerical determination of the temperature distribution, $T(r, t)$, inside the particle using the finite-difference method [6–8].

In practical plasma spraying one does not need to know the complete temperature function, $T(r, t)$, it is enough to know the time-dependent position of the phase boundary, $\eta(t)$ and the temperature at the particle surface, $T_s(t)$ during the dwell time. The surface temperature of the particles can even be measured [9, 10], so that the calculated results can be compared to the measured values.

In this paper we give the equations of the phase boundary position, $\eta(t)$, the particle surface temperature and their numerical solutions for some cases because this way seems to be simpler than the computation of $T(r, t)$ inside the particle.

In order to describe the melting of particles we have to know the temperature and velocity distribution in the plasma jet, because knowing them the motion of powder grains and the plasma temperature seen by the particle can be determined as a function of time. In this paper the description of the particle motion is given by taking into account the dependence of the temperature and velocity on position and of the viscosity and density on temperature. Scott and Cannel [11] made calculations with similar conditions for the particle motion in plasma.

2. EQUATION OF POSITION OF PHASE BOUNDARY

2.1. *Constant heat transfer coefficient*

We have used the following assumptions:

(i) The effect of convection as a heat transfer process in the liquid phase is neglected.
(ii) The particles have spherical symmetry.
(iii) The material constants of powder grains (C_p, ρ, κ) can be represented by their mean values.

The temperature distribution within the particle is governed by the equation

$$\rho C_p \frac{\partial T}{\partial t} - \frac{\kappa}{r}\frac{\partial^2}{\partial r^2}(rT) = 0 \qquad (2)$$

with the boundary condition due to the heat balance equation at the particle surface, i.e.

$$\kappa \frac{\partial T}{\partial r} = \alpha(T_g(t) - T)|_{r=r_0} \qquad (3)$$

where α is the heat transfer coefficient and $T_g(t)$ is the temperature experienced by the particle.

The symmetry condition in the centre of a particle can be written as

$$\left.\frac{\partial T}{\partial r}\right|_{r=0} = 0. \qquad (4)$$

Another boundary condition is due to the heat balance at the moving solid/liquid interface and can be written in the form:

$$\kappa \left.\frac{\partial T}{\partial r}\right|_{r=\eta(t)-0} - \kappa \left.\frac{\partial T}{\partial r}\right|_{r=\eta(t)+0} = L\rho \frac{d\eta}{dt}\theta(t-t_0) \qquad (5)$$

where L is the latent heat of fusion, $\theta(x)$ the Heaviside function and t_0 is the time when the surface temperature

NOMENCLATURE

C_D drag coefficient
C_p specific heat
D diameter of powder grain
F' non-dimensional temperature
F_0 non-dimensional gas temperature
L latent heat of fusion
m_p mass of particle
Nu Nusselt number
Pr Prandtl number
q heat flux
r radial coordinate
r_0 radii of particle
Re Reynolds number
t time
T temperature
x' non-dimensional radial coordinate, r/r_0
z cylindrical coordinate.

Greek symbols
α heat transfer coefficient
β non-dimensional solid/liquid interface, $\eta(t)/r_0$
$\eta(t)$ solid/liquid interface position
$\mu(T)$ viscosity
κ thermal conductivity
ρ density
τ non-dimensional time, $t \cdot \kappa/\rho C_p r_0^2$.

Subscripts
g gas
s surface
r room.

of the particle has just reached the melting point, i.e.

$$T(r_0, t_0) = T_m. \tag{6}$$

Finally, the temperature at the solid/liquid interface is equal to the melting point, i.e.

$$T(\eta(t), t) = T_m. \tag{7}$$

The heat transfer equation (2) and the boundary condition (5) can be written in a single equation introducing a heat source by the definition

$$q = L\rho \frac{d\eta}{dt} \theta(t-t_0)\delta(r-\eta(t)) \tag{8}$$

where δ is the Dirac δ function. With the use of this expression, equations (2) and (5) can be written as

$$\rho C_p \frac{dT}{dt} - \frac{\kappa}{r}\frac{\partial^2}{\partial r^2}(rT) = q. \tag{9}$$

Let us introduce the dimensionless variables

$$x = \frac{r}{r_0} \tag{10}$$

$$\tau = \frac{t\kappa}{\rho C_p r_0^2} \tag{11}$$

$$\beta(\tau) = \frac{\eta(t)}{r_0} \tag{12}$$

$$F_0(\tau) = \frac{C_p}{L}(T_g(t) - T_m) \tag{13}$$

$$F_m = \frac{C_p}{L}(T_m - T_r) \tag{14}$$

$$F'(x, \tau) = \frac{C_p}{L}(T(r, t) - T_m)x \tag{15}$$

and the Nusselt number

$$Nu = \frac{\alpha r_0}{\kappa}. \tag{16}$$

Using these quantities the equations (3), (4), (6) and (7) get the following forms:

$$\frac{\partial F'}{\partial \tau} - \frac{\partial^2 F'}{\partial x^2} \theta(\tau-\tau_0)x\frac{d\beta}{d\tau}\delta(x-\beta(\tau)) \tag{17}$$

$$\frac{\partial F'}{\partial x} = (1-Nu)F' + Nu\,F_0(\tau)|_{x=1} \tag{18}$$

$$F'(0, \tau) = 0 \tag{19}$$

$$F'(1, \tau_0) = 0 \tag{20}$$

$$F'(\beta(\tau), \tau) = 0. \tag{21}$$

To solve these equations let us suppose the solution in the form

$$F' = F + Nu\,F_0(\tau)f(x) \tag{22}$$

where $f(x)$ is defined by

$$f(x) = \begin{cases} \dfrac{(1-\varepsilon-x)^2}{2\varepsilon-(1-Nu)\varepsilon^2} & \text{if} \quad x > 1-\varepsilon \\ 0 & \text{if} \quad 0 \leqslant x \leqslant 1-\varepsilon. \end{cases} \tag{23}$$

This function is shown in Fig. 1. If $\varepsilon \ll 1$ then $f(1) \approx \varepsilon/2$.

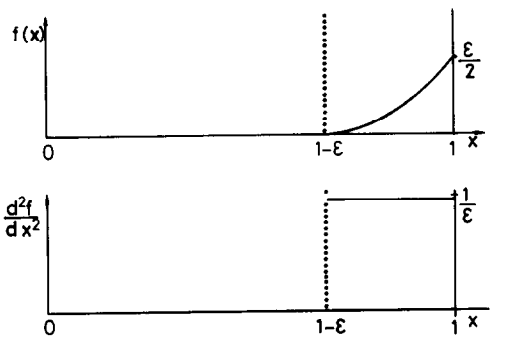

FIG. 1. The $f(x)$ and d^2f/dx^2 functions (see text).

The second derivative of $f(x)$ is given by

$$\frac{d^2f}{dx^2} = \begin{cases} \dfrac{2}{2\varepsilon-(1-Nu)\varepsilon^2} \approx \dfrac{1}{\varepsilon} & \text{if } x > 1-\varepsilon \\ 0 & \text{if } 0 \leqslant x \leqslant 1-\varepsilon. \end{cases}$$

It can be seen that $f(x) \ll d^2f/dx^2$ if $\varepsilon \ll 1$. Substituting F' into (17)–(19) we get

$$\frac{\partial F}{\partial \tau} - \frac{\partial^2 F}{\partial x^2} = \theta(\tau-\tau_0)x\frac{d\beta}{d\tau}\delta(x-\beta(\tau)) + Nu\,F_0\frac{d^2f}{dx^2} = G(x,\tau) \quad (24)$$

$$\frac{\partial F}{\partial x} = (1-Nu)F|_{x=1} \quad (25)$$

$$F(0,\tau) = 0 \quad (26)$$

Using the complete orthonormal system

$$U_n(x) = \sin k_n x \cdot \left(\int_0^1 \sin^2 k_n x\,dx\right)^{-1/2}. \quad (27)$$

F can be given by

$$F(x,\tau) = \sum_{n=0}^{\infty} C_n(\tau)U_n(x). \quad (28)$$

Because of the boundary conditions (25) and (26), k_n satisfies the equation

$$\frac{1}{1-Nu}k_n = \tan(k_n), \quad (29)$$

the graphic solution of which is shown in Fig. 2. Multiplying equation (24) by $U_n(x)$ and integrating between 0 and 1 and taking $\varepsilon \to 0$ we get the following equation for $C(\tau)_n$

$$\frac{dC_n}{d\tau} + k_n^2 C_n = \theta(\tau-\tau_0)\beta(\tau)\frac{d\beta}{d\tau}U_n(\beta(\tau)) + Nu\,F_0(\tau)u_n(1) = G_n(\tau). \quad (30)$$

Its solution is

$$C_n(\tau) = \left\{C_n(0) + \int_0^\tau G_n(t)\,e^{k_n^2 t}\,dt\right\}e^{-k_n^2\tau}. \quad (31)$$

where $C_n(0)$ can be determined from the initial condition. If $T(r,0) = T_r$ then

$$C_n(0) = \int_0^1 F(x,0)U_n(x)\,dx = -\frac{F_n\,Nu}{k_n^2}U_n(1). \quad (32)$$

Using (28) and (31) we get $F(x, t)$ as a function of $\beta(\tau)$ which can be given by using condition (21) as

$$\sum_{n=0}^{\infty} U_n(\beta(\tau))C_n(\tau) = 0. \quad (33)$$

Introducing the quantity

$$A(x, x_0, t) = \sum_{w=0}^{\infty} U_n(x)U_n(x_0)\,e^{-k_n^2 t} \quad (34)$$

and using equation (31), equation (33) leads to the following integro-differential equation:

$$\int_0^1 F(x,0)A(x,\beta(\tau),\tau)\,dx + \int_{\tau_0}^{\max\{\tau,\tau_0\}} \beta(t)\frac{d\beta}{dt}A(\beta(t),\beta(\tau),\tau-t)\,dt + \int_0^\tau Nu\,F_0(t)A(1,\beta(t),\tau-t)\,dt = 0. \quad (35)$$

On the basis of equations (28) and (31) the surface temperature is given by

$$F(1,\tau) = \int_0^1 F(x,0)A(x,1,\tau)\,dx + \int_{\tau_0}^{\max\{\tau,\tau_0\}} \beta(t)\frac{d\beta}{dt}A(\beta(t),1,\tau-t)\,dt + \int_0^\tau Nu\,F_0(t)A(1,1,\tau-t)\,dt \quad (36)$$

τ_0 can be determined from the implicit equation,

$$F(1,\tau_0) = 0.$$

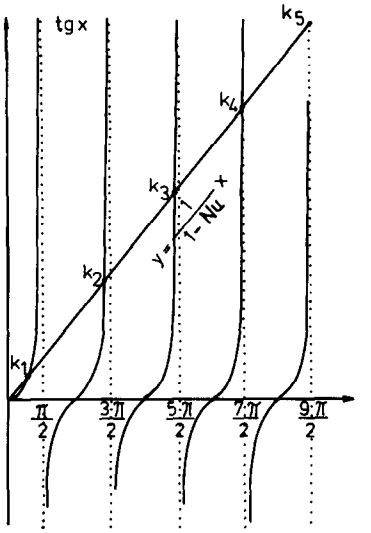

FIG. 2. The solution of the transcendent equation (29).

2.2. *Temperature-dependent heat transfer coefficient*

In the previous section the heat transfer coefficient, α, was supposed to be constant but α usually depends strongly on the plasma temperature. The integrated thermal conductivity of the plasma gas $\bar{\kappa}_g$ is defined by

$$\bar{\kappa}_g = (T_g - T_s)^{-1}\int_{T_s}^{T_g} \kappa_g(T)\,dT$$

Ranz and Marshall [10] give the following approximation for α

$$\alpha = \bar{\kappa}_g(2+0.6Re^{1/2}\,Pr^{1/3})/2r_0.$$

If the Reynolds number is not too high, then $\alpha = \bar{\kappa}_g/r_0$

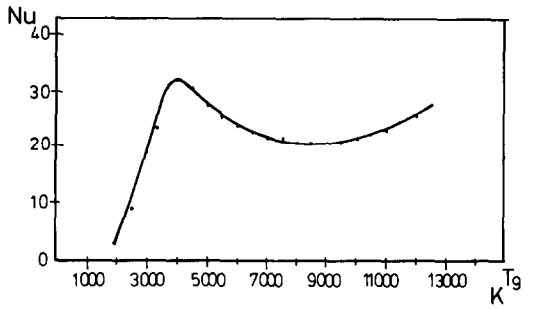

FIG. 3. The Nusselt number as a function of plasma temperature for alumina particles in an Ar–H_2 plasma.

so the Nusselt number

$$Nu = \frac{\bar{\kappa}_g}{\kappa}.$$

Using the data given in the literature [14, 15] the connection between Nu and the plasma temperature, T_g for alumina particles in Ar–H_2 plasma is shown in Fig. 3. These values of the Nusselt number were used in the numerical calculations discussed in Section 3. Taking into account that the heat transfer coefficient depends on temperature, $\alpha(T_g)$ can be approximated by a step function $\bar{\alpha}(T_g)$. In the intervals where the step function is constant equation (35) remains still valid with exchanging the variables $F(x, 0) \to F(x, \tau_n)$ and taking $\tau_0 \to \max\{\tau_0, \tau_n\}$ where τ_n is the time moment of the discontinuity of $\bar{\alpha}(T_g(\tau))$. The denotation $\tau_0 \to \max\{\tau_0, \tau_n\}$ means that τ_0 must be exchanged by the maximum value element of the set $\{\tau_0, \tau_n\}$. So equation (35) is given in each interval $\tau_n < \tau < \tau_{n+1}$ by

$$\int_0^1 F(x, \tau_n) A_n(x, \beta(\tau), \tau)\,dx + \int_{\max\{\tau_n, \tau_0\}}^{\max\{\tau, \tau_n, \tau_0\}} \beta(t) \frac{d\beta}{dt} A(\beta(t), \beta(\tau), \tau - t)\,dt + \int_{\tau_n}^{\tau} Nu_n F_0(t) A_n(x, \beta(t), \tau - t)\,dt. \quad (37)$$

The index n denotes the intervals where the value of the Nusselt number is Nu_n. The surface temperature distribution is then given by

$$F(x, \tau) = \int_0^1 F(\tau_n, x_0) A(x, x_0, \tau)\,dx_0 + \int_{\max\{\tau_n, \tau_0\}}^{\max\{\tau, \tau_n, \tau_0\}} \beta(t) \frac{d\beta}{dt} A_n(x, \beta(t), \tau - t)\,dt + \int_{\tau_n}^{\tau} Nu_n F_0(t) A_n(x, 1, \tau - t)\,dt \quad (38)$$

where $\beta(\tau)$ has to be calculated from equation (37).

3. NUMERICAL RESULTS

3.1. *Plasma parameters*

In the numerical calculations the melting of the particles was investigated by using the temperature and velocity distribution in an Ar–H_2 plasma jet measured by Vardelle *et al.* [7] (Fig. 4). The power of the plasma generator was 29 kW with a flow rate of 75 Nl min^{-1} of Ar and of 37 Nl min^{-1} of H_2. The dependence of the viscosity of the Ar–H_2 plasma on temperature was approximated between 2000 and 12 000 K by an analytical function using the data given in ref. [14]:

$$\eta(T) = \eta_0 \exp\left(-\frac{T - T_1}{T_2}\right)^a$$

where T_1, T_2, η_0 and a are constants (Fig. 5).

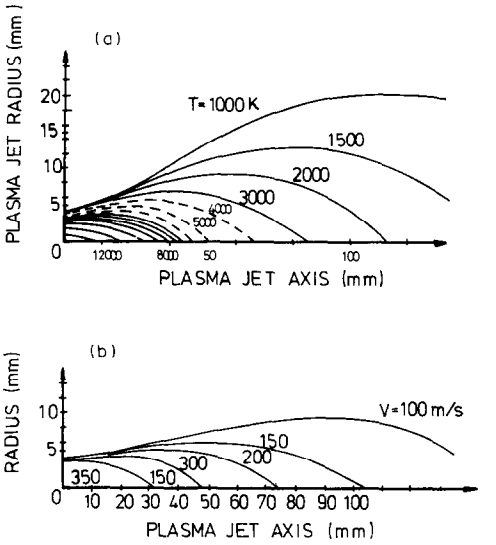

FIG. 4. Temperature (a) and axial velocity (b) isocontours of an argon hydrogen DC plasma jet at $P = 29$ kW, $D_{Ar} = 75$ Nl min^{-1}, $D_{H_2} = 37$ Nl min^{-1}.

3.2. *The motion of the particles*

The equation of particle motion in plasma has the following form according to the Stokesian law

$$m_p \frac{d^2 r}{dt^2} = \frac{8}{\pi} D^2 \rho_g C_D (\mathbf{V}_g - \mathbf{V}) |\mathbf{V}_g - \mathbf{V}| \quad (39)$$

where m_p, D, $\mathbf{V}$ are the mass, diameter and velocity of the particle and ρ_g, $\mathbf{V}_g$ are the density and velocity of the plasma and the dimensionless C_D is the drag coefficient. The connection between C_D and the Reynolds number

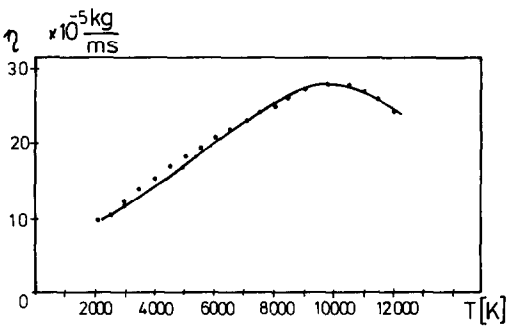

FIG. 5. The dependence of viscosity of Ar–H_2 plasma on temperature.

was taken from the work of Beard and Pruppacher [13]:

$$C_D = \frac{24}{Re} g(Re) \tag{40}$$

where

$$g(Re) = \begin{cases} 1 & \text{if } Re < 0.2 \\ 1+0.1\,Re^{0.99} & \text{if } 0.2 \leqslant Re < 2 \\ 1+0.11\,Re^{0.81} & \text{if } 2 \leqslant Re < 21 \\ 1+0.189\,Re^{0.63} & \text{if } 21 \leqslant Re < 200. \end{cases}$$

The numerical values for Re are calculated by the well known formula

$$Re = \frac{|\mathbf{V}_g - \mathbf{V}|\, D\rho_g}{\eta}.$$

In the equation of motion we have neglected the Basset history term, because it causes no significant difference [12]. It has to be mentioned that the correction term for C_D used by Lewis and Gauvin [12] is unnecessary if the temperature dependence of the plasma properties is taken into account.

The equation of motion (39), can be rewritten in cylindrical co-ordinates z, r. Using (40) and the fact that the radial component of the velocity v_g is much less than the axial velocity component u_g of the plasma we get

$$\frac{dz^2}{dt^2} = \frac{18\eta(T_g(z,r))}{D^2\rho}\left[U_g(z,r) - \frac{dz}{dt}\right] g(Re) \tag{41}$$

$$\frac{dr^2}{dt^2} = \frac{18\eta(T_g(z,r))}{D^2\rho}\frac{dr}{dt} g(Re). \tag{42}$$

The differential equations (41), (42) have been solved by the Runge–Kutta method. The particle diameter was varied between 10 and 100 μm. The initial conditions for the particle motion are $z(0) = 0$ and $r(0) = 4$ mm. The initial velocity of the particles was taken to be perpendicular to the axis, and its values were chosen as 5, 10 and 15 m s^{-1}.

Figure 6 shows the trajectories of the particles with different diameters at an initial velocity of 15 m s^{-1}. The curves $T_g(t)$ at particle diameters of 80, 90 and 100 μm are shown in Figs. 7(a)–(c).

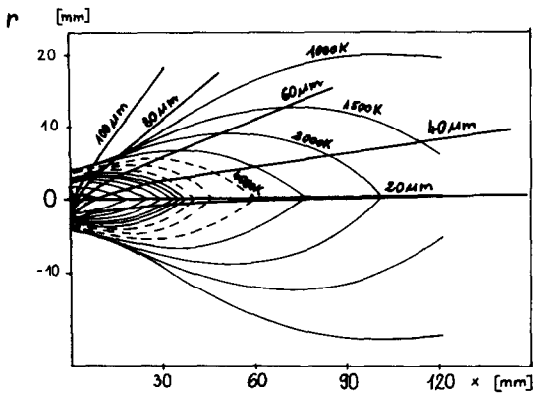

FIG. 6. Trajectories of the alumina particles with different diameters in an Ar–H_2 plasma jet. The injection velocity is 15 m s^{-1}.

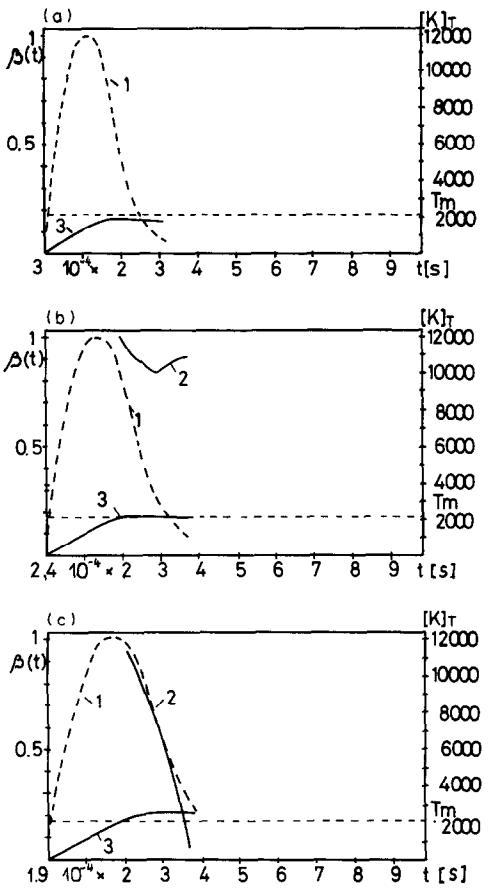

FIG. 7. Calculated positions of the solid/liquid interface in a particle and its surface temperature during its flight through an Ar–H_2 plasma jet as function of time. The particle diameters are (a) 100 μm, (b) 90 μm and (c) 80 μm. The curves 1 show the plasma temperature seen by the particle, the curves 2 show the position of the solid/liquid interface and curves 3 show the surface temperature of the particle.

3.3. *Numerical calculations of the solid/liquid interface position*

If the plasma temperature $T_g(t)$ seen by the particle in the plasma is known, then equation (37) can be solved numerically. Figure 7 shows a few results which are due to particles with different degrees of melting.

The particle injected with a velocity of 15 m s^{-1} and a diameter of 100 μm does not begin to melt. The particle with a diameter of 90 μm melts partly, after which it becomes solid again in the plasma. The particle with a diameter of 80 μm melts completely in the plasma.

In Fig. 7 the curves 1 always show the plasma temperature seen by the particle, the curves 2 show the position of the solid/liquid interface and curves 3 show the surface temperature of the powder particle as a function of time. The time units of the three curves are not equal.

4. CONCLUSION

To describe the melting of a powder particle flying through a plasma jet an integro-differential equation of motion of the melting front inside the particle can be determined. This equation contains the time-dependent plasma temperature seen by the particle as a boundary condition. To determine this temperature one needs to investigate the particle motion in a plasma. The equation of motion is given according to the Stokesian law and the temperature dependence of the plasma viscosity can also be taken into account. In a few special cases the equations can be solved numerically and the solution gives the melting front position and the surface temperature of the powder particle as a function of time.

Acknowledgement–The authors are grateful to Professor I. Kovács and to Dr L. Brájer for their valuable discussions of this work.

REFERENCES

1. J. L. Engelke, Paper presented at Meeting of the American Institute of Chemical Engineers, Los Angeles (January 1962).
2. D. R. Mash, N. E. Weare and D. L. Walker, *J. Met.* **13,** 473 (1961).
3. D. Apelian, M. Maliwal, R. W. Smith and W. F. Schilling, *Int. Met. Rev.* **28,** 271 (1983).
4. Wi Chen and E. Pfenden, *Plas. Chem. Plas. Proc.* **2,** 293 (1982).
5. J. M. Houben, In *9th International Thermal Spray Conference* (edited by A Vardelle *et al.*), p. 143. Netherland Institute voon Lastechneik, The Hague (1980).
6. T. Yosida and K. Akashi, *J. appl. Phys.* **48,** 2252 (1977).
7. A. Vardelle, M. Vardelle and P. Fauchais, *Plas. Chem. Plas. Proc.* **2,** 255 (1982).
8. J. K. Fiszdon, *Int. J. Heat Mass Trans.* **22,** 749 (1978).
9. B. Kruszewska et J. Lesinski, *Revue de Phys. appl.* **12,** 1203 (1977).
10. W. E. Rane and W. R. Marshall, *Chem. Engng Prog.* **48,** 141 (1952).
11. B. F. Scott and J. K. Cannel, *Int. J. Mach. Tool. Des. Res.* **7,** 243 (1967).
12. J. A. Lewis and W. H. Gauvin, *A.I.Ch.E. Jl* **19,** 982 (1973).
13. K. V. Beard and H. R. Pruppacher, *J. atmos. Sci.* **26,** 1066 (1969).
14. A. V. Donskoi and V. S. Klubnikin, Elektroplazmennye protzessy i ustanovki v mashinostroenii, *Mashinostroenie,* Leningrad (1979).
15. V. H. Yureneva and P. D. Lebedeva (Editors), *Teplotehnicheski sparvoshnik,* Vol. 1. Energiya, Moscow (1975).

FUSION DE GRAINS DE POUDRE DANS UN JET DE PLASMA

Résumé—Un modèle numérique de la fusion de petites particules qui entrent dans un jet de plasma est étudié pour prédire les paramètres optimaux de la dispersion du plasma. L'équation du mouvement pour l'interface solide/liquide dans une particule qui passe à travers un jet de plasma est déterminée et sa solution numérique est donnée dans quelques cas particuliers. La forte variation de température et de vitesse dans le jet de plasma et la dépendance à la température des paramètres du plasma sont prises en compte.

DAS SCHMELZEN VON STAUBKÖRNERN IM PLASMASTRAHL

Zusammenfassung—Zur Vorhersage der optimalen Parameter eines Plasmastrahls wurde ein numerisches Modell vom Schmelzen kleiner Teilchen, die einem freien DC-Plasmastrahl zugeführt werden, erarbeitet. Die Bewegungsgleichung für die Grenzfläche fest/flüssig innerhalb eines Teilchens, das einen Plasmastrahl durchquert, wurde bestimmt und die numerische Lösung davon in einigen speziellen Fällen angegeben. Die starke Temperatur- und Geschwindigkeitsänderung innerhalb des Plasmastrahls und die Temperaturabhängigkeit der Plasma-Einflußgrößen wurden berücksichtigt.

ПЛАВЛЕНИЕ ТВЕРДЫХ ЧАСТИЦ ПРИ ПЛАЗМЕННОМ РАСПЫЛЕНИИ

Аннотация—Для расчета оптимальных параметров плазменного распыления исследуется численная модель плавления малых частиц, попадающих в свободную струю плазмы, получаемую нагревом газа постоянным током. Найдено уравнение движения границы раздела фаз для частицы, нагреваемой плазменной струей, а его численное решение дано для некоторых частных случаев. Учитывались сильные изменения температуры и скорости в плазменной струе и зависимость параметров плазмы от температуры.